

Novel demonstration of RNAi in citrus reveals importance of citrus callose synthase in defence against *Xanthomonas citri* subsp. *citri*

Ramón Enrique¹, Florencia Siciliano¹, María Alejandra Favaro¹, Nadia Gerhardt¹, Roxana Roeschlin¹, Luciano Rigano², Lorena Sendin³, Atilio Castagnaro³, Adrian Vojnov² and María Rosa Marano^{1*}

¹Instituto de Biología Molecular y Celular de Rosario (IBR-CONICET). Área Virología, Facultad de Ciencias Bioquímicas y Farmacéuticas, Universidad Nacional de Rosario. Suipacha, Rosario, Argentina

²Fundación Pablo Cassará, Centro de Ciencia y Tecnología "Dr. Cesar Milstein". Saladillo. Ciudad de Buenos Aires, Argentina

³Estación Experimental Agroindustrial Obispo Colombres, Las Talitas, Tucumán, Argentina

Received 22 April 2010;

revised 7 July 2010;

accepted 8 July 2010.

*Correspondence (fax 54-341-4390465;
email marano@ibr.gov.ar)

Summary

Citrus is an economically important fruit crop that is severely afflicted by citrus canker, a disease caused by the bacterial phytopathogen, *Xanthomonas citri* subsp. *citri* (Xcc). GenBank houses a large collection of Expressed Sequence Tags (ESTs) enriched with transcripts generated during the defence response against this pathogen; however, there are currently no strategies in citrus to assess the function of candidate genes. This has greatly limited research as defence signalling genes are often involved in multiple pathways. In this study, we demonstrate the efficacy of RNA interference (RNAi) as a functional genomics tool to assess the function of candidate genes involved in the defence response of *Citrus limon* against the citrus canker pathogen. Double-stranded RNA expression vectors, encoding hairpin RNAs for citrus host genes, were delivered to lemon leaves by transient infiltration with transformed *Agrobacterium*. As proof of principle, we have established silencing of citrus phytoene desaturase (*PDS*) and callose synthase (*CaLS1*) genes. Phenotypic and molecular analyses showed that silencing vectors were functional not only in lemon plants but also in other species of the *Rutaceae* family. Using silencing of *CaLS1*, we have demonstrated that plant cell wall-associated defence is the principal initial barrier against *Xanthomonas* infection in citrus plants. Additionally, we present here results that suggest that H₂O₂ accumulation, which is suppressed by xanthan from Xcc during pathogenesis, contributes to inhibition of xanthan-deficient Xcc mutant growth either in wild-type or *CaLS1*-silenced plants. With this work, we have demonstrated that high-throughput reverse genetic analysis is feasible in citrus.

Keywords: RNAi-induced gene silencing, citrus functional genomics, *Xanthomonas citri* subsp. *citri*, asiatic citrus canker, callose synthase.

Introduction

Citrus is the most economically significant fruit tree crop in the world, with an annual production of 105 million tons. Lemon, classified as *Citrus limon* (L.) Burm. f. (Tanaka, 1969) is the third most important *Citrus* species after orange and mandarin. The Tucumán Province of Argentina is one of the world's largest lemon producers, with an annual output of approximately 1.47 million tons. A high percentage (60%) of its production is designated

for industry processing (elaboration of concentrated juice, essential oils and dried lemon peels) and the rest is commercialized as fresh fruit (<http://www.fas.usda.gov/currwmt.asp/Citrus>: World Markets and Trade). Production satisfies domestic fresh lemon fruit demand throughout the year and generates a surplus that is sold to meet the off-season demands of markets in the northern hemisphere.

Asiatic citrus canker is caused by *Xanthomonas axonopodis* pv. *citri* (Xac), recently renamed *Xanthomonas citri*

subsp. *citri* (Xcc) (Schaad *et al.*, 2006), which is the most severe and wide-spread bacterial pathogen to afflict citrus (Graham *et al.*, 2004). Most of the world's commercial citrus cultivars are moderately to highly susceptible to Xcc, and once established, the pathogen is difficult to eradicate. Quarantine is used to prevent spread to new geographic regions. Disease management options are currently limited to the use of copper-based bactericides, destruction of diseased trees and surrounding areas, and replacement with less susceptible cultivars where possible (Graham *et al.*, 2004).

There is great need for new and sustainable strategies to manage asiatic citrus canker. Field evaluations suggest that full or partial resistance to Xcc does exist among several types of citrus and closely related genera, including *Citrus ichangensis*, *C. junos*, *C. medica*, *C. unshiu*, *Citrofortunella* and *Fortunella* spp (Schubert *et al.*, 2001; Lee *et al.*, 2009; Shiotani *et al.*, 2009). However, characterization of this resistance has only recently begun (Khalaf *et al.*, 2007; Lee *et al.*, 2009; Shiotani *et al.*, 2009). The other option, cultivar improvement through traditional breeding continues to be a difficult process, obstructed by apomixes, sexual incompatibility, prolonged juvenility, high heterozygosity and the complex hybrid nature of citrus. In fact, the citrus cultivars with the greatest worldwide economic significance (e.g. *C. sinensis*, *C. paradisi*, and *C. limon*) are not biologically defined species, but are rather the result of accumulated somatic mutation or natural hybridization in the wild places or field (Gmitter, 1995).

Biotechnology offers an alternate strategy for sustainable management of asiatic citrus canker, and citrus genomics is providing new tools for crop improvement. A large database of Expressed Sequence Tags (~559 000 ESTs) has recently been generated from a variety of *Citrus* species (International Citrus Genome/Genomics Consortium, <http://www.citrusgenome.ucr.edu/>), covering a wide range of tissues, developmental stages, and abiotic and biotic stress conditions (Forment *et al.*, 2005; Targon *et al.*, 2007; Terol *et al.*, 2007; Martinez-Godoy *et al.*, 2008; Marques *et al.*, 2009). In citrus, gene expression associated with pathogen response has been analysed in fungal (leaf spot, *Alternaria*; green mould, *Penicillium digitatum*; postbloom fruit drop, *Colletotrichum acutatum*; root rot, *Phytophthora parasitica*), bacterial (canker, *Xanthomonas* spp.; citrus variegated chlorosis, *Xylella fastidiosa*) and viral diseases [citrus tristeza virus (CTV); citrus leprosis virus (CiLV)] (Lahey *et al.*, 2004; Marcos *et al.*, 2005; Campos *et al.*, 2007; Cristofani-Yaly *et al.*, 2007;

Freitas-Astua *et al.*, 2007; Gandia *et al.*, 2007; Khalaf *et al.*, 2007; Souza *et al.*, 2007a,b; Targon *et al.*, 2007; Cernadas *et al.*, 2008).

Although candidate genes for citrus improvement have been identified and selected from these data, a significant number of unigenes (~15–20%) are unique to *Citrus* species and their biological functions have yet to be determined (Forment *et al.*, 2005; Martinez-Godoy *et al.*, 2008). RNA interference (RNAi) of plant genes, initiated by the delivery of double-stranded RNA (dsRNA) (Wesley *et al.*, 2001; Helliwell and Waterhouse, 2003), is an attractive forward and reverse genetic tool for the study of gene function in polyploidy species as citrus plants. In this work, we have tested the use of RNA silencing in *C. limon* plants based on RNAi technology, using an intron-containing self-complementary 'hairpin' RNA (hpRNAi) construct (Helliwell and Waterhouse, 2003). To induce silencing, dsRNAs were delivered by infiltrating lemon leaves with *Agrobacterium tumefaciens* carrying the hpRNAi-transgene. Two target genes have been analysed: citrus phytoene desaturase (*PDS*) and citrus callose synthase (*CaLS*) (Verma and Hong, 2001), also referred as glucan synthase-like (*GSL*) (Richmond and Somerville, 2000). The *PDS* gene was selected as a control. Its reduction confers a clear photobleaching phenotype on the leaves, and it has been used successfully as a control in several RNA silencing systems (Kumagai *et al.*, 1995; Ruiz *et al.*, 1998; Liu *et al.*, 2002; Brigneti *et al.*, 2004).

Callose is the predominant cell wall polysaccharide, consisting of β -1,3-glucan chains, present in the nascent cell plate during normal plant growth and development (Samuels *et al.*, 1995; Thiele *et al.*, 2009) and is also involved in response to biotic and abiotic stress (for a recent review see Chen and Kim, 2009). Callose is synthesized by callose synthases, which are membrane-bound enzymes that have been relatively well characterized in *Arabidopsis* (Chen and Kim, 2009). Most information on callose in plants comes from analysis of *CaLS/GSL* knockout mutations in *Arabidopsis*, which has 12 putative *CaLS/GSL* genes (Vogel and Somerville, 2000; Jacobs *et al.*, 2003; Nishimura *et al.*, 2003; Dong *et al.*, 2008; Thiele *et al.*, 2009). It has been suggested that multiple *CaLS* genes may have evolved in higher plants for the synthesis of callose in different locations and in response to different physiological and developmental signals (Verma and Hong, 2001; Nishimura *et al.*, 2003; Enns *et al.*, 2005; Thiele *et al.*, 2009). The regulation of *CaLS* genes expression during plant development and after pathogen infection has recently been reported in *Arabidopsis* (Dong *et al.*, 2008). Callose

synthase was chosen as an RNAi silencing target in this study because callose plays a role in key plant processes, but the nature and function of *CalS* genes have yet to be fully characterized in citrus. The *C. limon* *CalS* sequence shares 83% identity with the *Arabidopsis* *CalS1/GSL6* catalytic subunit, which is located at the growing cell plate, interacts with cell plate-associated proteins (Hong *et al.*, 2001) and is induced in response to pathogen attack (Dong *et al.*, 2008). We hypothesized that the loss of *CalS1* function through RNAi silencing in citrus would produce altered leaf morphology. Given that previous work has indirectly implicated callose deposition in the resistance of host plants to infection by *Xanthomonas campestris* pv. *campestris* (Yun *et al.*, 2006), we decided to examine the influence of *CalS1* silencing on the outcome of this *Citrus*-*Xcc* interaction. Our results demonstrate that plant cell wall-associated defence is the principal initial barrier against *Xanthomonas* infection in citrus plants and that callose deposition and H₂O₂ accumulation in *C. limon*, which is suppressed by *Xanthomonas citri* subsp. *citri* during pathogenesis, contributes to inhibition of xanthan-deficient *Xcc* *gumB* mutant in both wild-type and *CalS1*-silenced plants.

Results

Testing the effectiveness of RNA silencing in *C. limon*

To examine whether hpRNA-derived siRNAs can be used to characterize gene function and manipulate the defence response to *Xanthomonas* in citrus plants, we first tested the efficiency and extent of RNA silencing in citrus using the endogenous lemon *PDS* gene. We chose this gene because loss of the *PDS* enzyme blocks carotenoid synthesis culminating in photo-oxidation of chlorophylls and a photobleaching phenotype that facilitates visual monitoring of silencing induction and progression (Kumagai *et al.*, 1995).

The *C. limon* *PDS* (*Cl-PDS*) sequence showed 100% identity with both orange *PDS* (gb/AY669082.1) and mandarin *PDS* (AB046992) genes. A binary hpRNA vector (pHG12 *Cl-PDS*) regulated by the 35S promoter was constructed from pHELLSGATE12 by replacing the *ccdB* coding region flanked by *attL* sites with the lemon *Cl-PDS* gene using Gateway technology (Figure 1a). The second pair of leaves of four- to six-leaf stage plants grown from seeds of *C. limon* cultivars Eureka Frost and Lisboa Frost were agro-infiltrated with two clones chosen at random, pHG12 *Cl-PDS*-F and pHG12 *Cl-PDS*-R (one construct per

plant, allowing for four vector-variety combinations). A representative four- to six-leaf stage plant is shown in Figure 1b. At 15–25 days postinoculation (dpi), symptoms of *PDS* silencing resulting from local RNAi induction were observed only in inoculated tissues (Figure 1c). At 60 dpi, 90% of the twenty agro-infiltrated plants showed some degree of silencing-induced photobleaching. Within a single plant, a varied degree of *PDS* silencing (RNAi*PDS*) was observed in uninoculated systemic leaves. Initially silencing was limited to regions surrounding the main veins (Figure 1d). Later as new leaves formed, we observed spread of *PDS* silencing across the whole leaf, indicating that the silencing signal moves between cells and over long distances. Strong silencing in test plants resulted in leaves that were almost completely white (Figure 1d, f). The leaves of control wild-type plants of either cultivar remained green after infiltration with *Agrobacterium* EHA105 alone (Figure 1e).

Quantitative reverse transcription-polymerase chain reaction (qRT-PCR) analysis showed that endogenous *PDS* mRNA levels were 64% lower in leaves showing strong photobleaching in pHG12 *Cl-PDS*-infiltrated plants compared to levels observed in control plants (data not shown).

We evaluated persistence of the phenotype for 6–12 months. Plants with a high degree of *PDS* silencing died after total photobleaching. Plants less severely affected recovered after losing photobleached leaves. Among the new growth, only some lateral leaves displayed photobleaching (Figure 1g). No clear difference in the silencing phenotype was observed among any of the four combinations of *PDS* vectors and citrus cultivars (data not shown).

Phenotype of the callose synthase silencing plants

We chose one putative EST sequence of the citrus callose synthase gene, *CalS/GSL*, from *C. reshni* (CX305437) to design primers to amplify a cDNA fragment of the *CalS/GSL* coding region of *C. limon* cv. Eureka. This EST sequence of *C. limon* *CalS1* (*Cl-CalS1*) shares homology with a number of *CalS/GSL* sequences from *Arabidopsis*. Among these, it most closely homologous with the published *Arabidopsis* *CalS1/GSL6* gene (AF237733) at 83% identity. In *Arabidopsis*, *CalS1* gene expression is regulated in a tissue-specific manner in leaves and root hairs and is induced by salicylic acid treatment and upon pathogen infection (Dong *et al.*, 2008).

cDNA was used to construct a hairpin RNAi vector targeted to silence the endogenous citrus *CalS1* gene

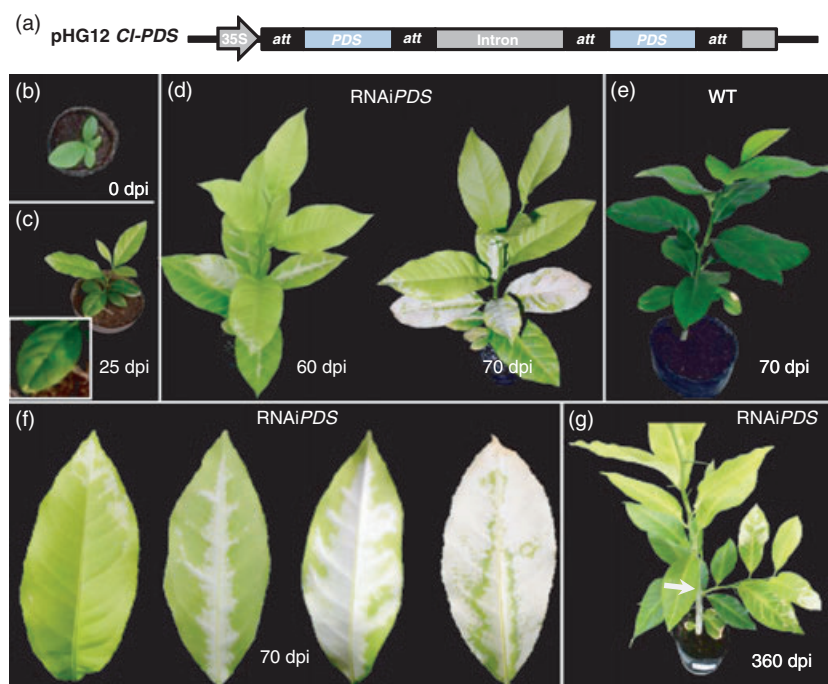


Figure 1 *Citrus limon* plants showing *PDS* silencing phenotype. (a) Schematic diagram of the pHG12 *CI-PDS* plasmid construct; 35S, CaMV 35S promoter; att, Gateway™ att sites (b) A plant at four-leaf stage agro-infiltrated with pHG12 *CI-PDS*. (c) The same plant at 25 days postinoculation (dpi), the agro-infiltrated leaf shows a close up (framed) of a *PDS*-silenced sector. (d) The same plant at 60 and 70 dpi, respectively. (e) Wild-type (WT) plants agro-infiltrated with bacteria (no vector) at 70 dpi. (f) Magnification of systemic leaves from plant displayed in (d), showing distinct *PDS* silencing phenotypes. In the first, leaf bleaching begins at the distal end; in the other, leaf bleaching begins from the central vein and extends to the periphery of the leaf from the secondary veins. (g) After pruning, a new branch sprouted maintaining the bleached phenotype (white arrow). Three independent biological assays were carried for each of the two cultivars (*C. limon* cv. Eureka Frost and *C. limon* cv. Lisboa Frost) and yielded similar results. In each assay, twenty lemon seedlings were used per cultivar, of which half were infiltrated with the transformed silencing vector and half were infiltrated with agrobacteria alone.

(pHG12 *CI-CalS1*). A suspension of *Agrobacterium* containing the pHG12 *CI-CalS1* construct (Figure 2a) was infiltrated into the second pair of leaves of four- to six-leaf stage plants grown from seeds of *C. limon* cv. Eureka. Approximately 5–10 days post-treatment, only the leaves infiltrated with pHG12 *CI-CalS1* developed a rough phenotype (Figure 2b). At 50 dpi, 100% of the 15 plants inoculated with the pHG12 *CI-CalS1* construct were noticeably shorter in height than the control wild-type plants, which showed a normal phenotype after inoculation with untransformed *Agrobacterium* (Figure 2c). The internode length of *CalS1*-silenced (RNAi*CalS1*) plants was shorter compared to those in wild-type plants (0.72 ± 0.088 cm vs. 1.4 ± 0.48 cm); however, the internode width and total number of nodes on the main stem were roughly the same in both plants (Figure 2c). The leaves of silenced plants were smaller on average than wild-type leaves and had a wrinkled texture, bumps and a heart shape (Figure 2d). These plants maintained the same phenotype 1-year post-treatment, indicating high silencing stability

during that period of time (Figure 2e). To determine whether the silencing phenotype could be propagated by grafting, RNAi*CalS1* plant scions were budded onto rootstocks of Troyer citrange (Figure 2f), another member of the *Rutacea* family. The propagation efficiency was >30%, and 80% of the regenerated shoot grafted shown the RNAi*CalS1* phenotype (Figure 2g).

To test whether citrus silencing methodology would work in other *Rutacea* species, we compared RNAi*CalS1* phenotypes on citrus and Troyer citrange seedling plants. The RNAi*CalS1* phenotypes were similar between the two *Rutacea* species. RNAi*CalS1* Troyer citrange plants were also markedly shorter in stature than the Troyer citrange control wild-type plants infiltrated with *Agrobacterium* EHA105 alone (Figure 2h), though the number of nodes was approximately the same. At 40–50 dpi, the new leaves from RNAi*CalS1* Troyer citrange plants were smaller than wild-type plants and appeared bilobular rather than trifoliar, which is characteristic Troyer citrange leaves (Figure 2h). We evaluated persistence of the phenotype

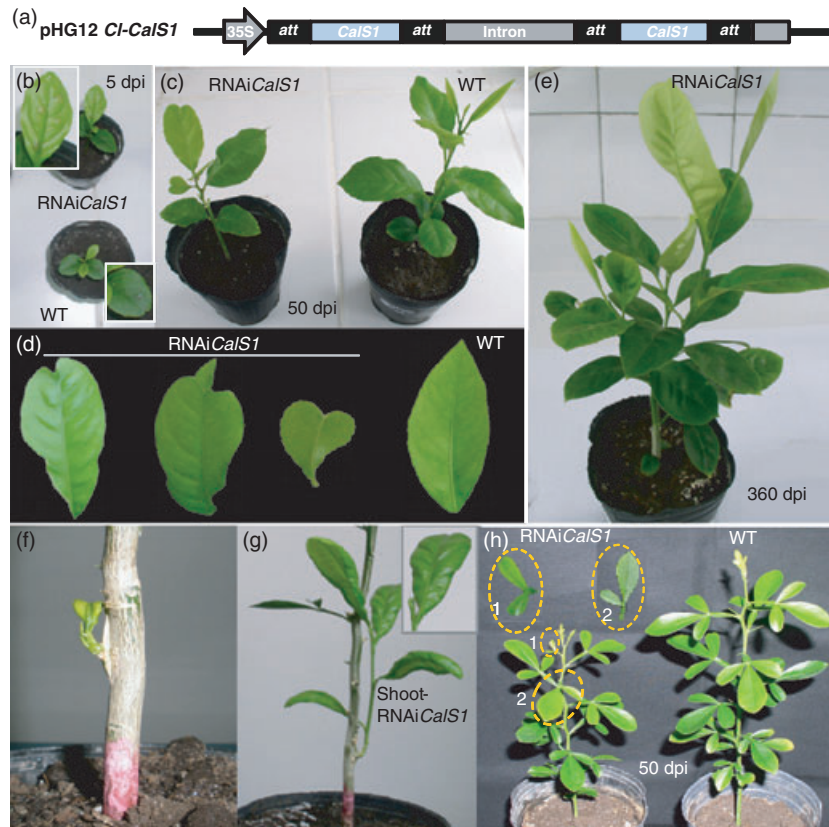


Figure 2 Phenotype of *CalS1* silencing in *Citrus limon* plants. (a) Schematic diagram of the pHG12 *CI-CalS1* construct; 35S, CaMV 35S promoter; att, Gateway™ att sites (b) Induction of *CalS1* silencing in agro-infiltrated lemon leaf with pHG12 *CI-CalS1* and wild-type (WT) plants agro-infiltrated with bacteria (no vector) at 5 days postinoculation (dpi). (c) The same RNAiCalS1 silencing plants after 50 dpi, WT plants at the same stage. (d) Systemic leaves with distinct *CalS1* silencing phenotypes from a single plant at 50 dpi and compared with the WT leaves. (e) *CalS1* silencing in *C. limon* after 360 dpi. (f) RNAiCalS1 lemon shoot grafted onto Troyer citrange rootstock at 20 days and (g) 5 months after budding, magnification of leaf phenotype (insert). (h) RNAiCalS1 silencing in Troyer citrange after 50 dpi. Areas within the dotted yellow lines show a bilobular phenotype in RNAiCalS1 leaves. Similar phenotypes were observed in 15 lemon and eight citrange plants analysed in at least three separate experiments.

for 15 months and 40% of the emerging leaves were bilobular in the RNAiCalS1 citrange plants (data not shown).

Histo-anatomic and molecular analysis of the RNAiCalS1 lemon leaves

Leaf anatomy of RNAiCalS1 lemon plants was analysed and compared with the leaf anatomy of wild-type plants. Wild-type leaves showed a highly organized structure (Figure 3a). The adaxial epidermis (AdE) was unilayered, regular in size, contained square shaped cells, and was covered by a thin and smooth cuticle. Dorsiventral mesophyll was differentiated into 2–3 layers of palisade parenchyma (PP) and several layers of spongy parenchyma (SP) cells, which were loosely arranged, with considerable intercellular spaces between them. The abaxial epidermis (AbE) was unstratified and contained square-shaped cells. Strikingly, the RNAiCalS1 leaves showed notches at the

epidermal level, and cells on both AdE and AbE were rectangular in shape, rather than square (Figure 3b). The mesophyll was disorganized; the PP cells appeared smaller than wild-type tissue cells and the spongy cells were tangentially flattened and more loosely arranged and dispersed than the wild-type plants.

We performed qRT-PCR to confirm suppression of endogenous *CalS1* mRNAs in *C. limon*, using accumulation of actin transcripts as an internal amplification control and for signal normalization. RNA samples from silenced and control plants were extracted at 60 dpi and amplified using primers specific to the target gene. Systemic leaves selected for the silenced sample, either from RNAiCalS1 plants or regenerated RNAiCalS1 shoot grafts, displayed strong phenotypic symptoms of callose synthase silencing. As shown in Figure 3c, *CalS1* mRNA levels were approximately 80% lower in silenced plants compared to control wild-type plants infiltrated with *Agrobacterium* EHA105 alone. These

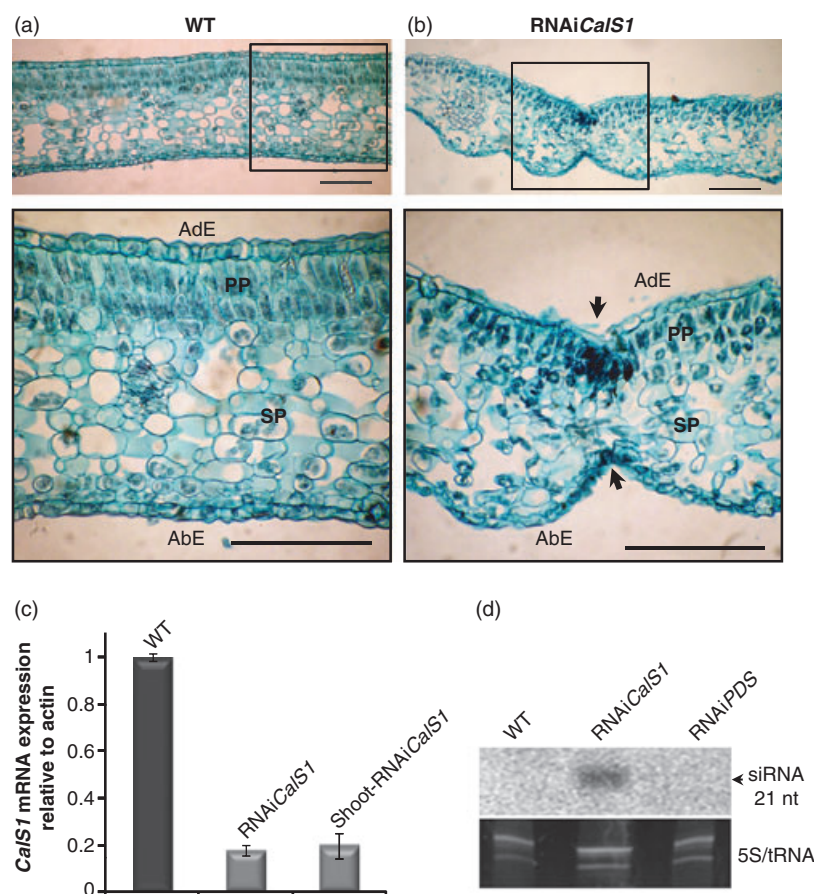


Figure 3 Anatomical structure and *CalS1* RNA levels in lemon leaves silenced with *CalS1*-hpRNAi. (a) A transversal section of a typical lemon wild-type (WT) leaf, magnification 20 \times . (b) Shortening of palisade cells and tangential flattening of spongy cells in RNAiCalS1-silenced leaf, magnification 20 \times . Insets show the amplification of the section tissue from figures a and b. AdE, adaxial epidermis; AbE, abaxial epidermis; PP, palisade parenchyma; SP, spongy parenchyma. Scale bar 100 μ m. Arrows show the notches in the AdE and AbE. (c) Quantitative RT-PCR analysis of the *CalS1* mRNA steady state levels in systemic RNAiCalS1 leaves. Average cycle threshold values and *n*-fold changes in gene expression in each silencing experiment compared to wild-type (WT) plants agro-infiltrated with bacteria (no vector) were calculated from triplicate samples. Error bars means \pm standard deviation of five independent RNAiCalS1 plants and four independent shoot grafted RNAiCalS1 plants. (d) Northern blot analysis for the detection of *CalS1* small interfering RNA (siRNA) accumulation levels in wild-type (WT), RNAiCalS1 and RNAiPDS plants at 60 days after agroinfiltration. Total RNA from systemic leaves was isolated and 15 μ g was blotted and probed with specific [α - 32 P] ATP-labelled DNA probes obtained by random priming from the *CalS1* sequences. The size of siRNAs was estimated using labelled 21 nucleotide synthetic RNAs. Ethidium bromide staining of the 5S/tRNA region of the gels is shown below as a loading control. Similar results were obtained with three independent sets of RNA extracts.

variations in *CalS1* transcripts levels correspond with the processing of the double-stranded RNA produced from hpRNA transgenes into 21 nt small interfering RNA (siRNA) in each of the silencing plants (Figure 3d). As expected, no accumulation of *CalS1* 21 nt siRNA was detected either in RNAiPDS or wild-type plants (Figure 3d).

Silencing *CalS1* makes citrus plant more susceptible to *Xcc*

We have previously provided evidence that callose is required for resistance to the bacterial pathogen, *Xanthomonas campestris* pv. *campestris*, and that xanthan, the

major exopolysaccharide secreted by *Xanthomonas* spp., induces susceptibility to *Xanthomonas campestris* pv. *campestris* in *N. benthamiana* and *Arabidopsis* by suppressing callose deposition (Yun *et al.*, 2006). Recently, we have shown that xanthan-defective mutants of *Xanthomonas axonopodis* pv. *citri* (*Xac* MgumB, renamed *Xcc* MgumB) are unable to cause disease in *C. limon* and that xanthan plays an important role in the formation of biofilms and in *Xcc* survival prior to development of canker (Rigano *et al.*, 2007), suggesting that callose may be required for resistance to *Xcc* as well.

To investigate this further, we inoculated young leaves of 60-day-old wild-type and RNAiCalS1 lemon plants with

bacterial suspensions of *MgumB* and wild-type *Xcc* at a concentration of 10^7 cfu/mL by cotton swab method. A green fluorescent protein (GFP)-labelled strain of *Xcc* and *MgumB* (Rigano *et al.*, 2007) were used to observe different stages of canker development. Forty-eight hours after infection, the inoculated leaves were stained for the presence of callose with aniline blue and observed by UV-fluorescence microscopy (Figure 4a, d). Callose deposition was visible in wild-type plants inoculated with *MgumB*, as indicated by the bright-light blue stain. No deposition was observed following inoculation with *Xcc* (Figure 4a). Thus, the reduced virulence of *MgumB* associated with the lack of xanthan correlates with callose deposition. Interestingly, RNAi*CaIS1* plants showed no callose deposition after infection with *MgumB* (Figure 4d), indicating that the *CaIS1* gene is also involved in pathogen recognition in citrus plant. As expected, we also observed no callose deposition when these silenced plants were infected with wild-type *Xcc* (Figure 4d).

At ten to fifteen dpi, leaves of wild-type plants inoculated with *Xcc* showed canker development while *MgumB* showed no symptoms, as has been demonstrated previously

(Rigano *et al.*, 2007) (Figure 4b). Interestingly, the canker symptoms in RNAi*CaIS1* plants were slightly stronger than in wild-type plants inoculated with *Xcc* (Figure 4b, e). Surprisingly, we observed canker development in *CaIS1*-silenced plants inoculated with *MgumB* (Figure 4e). However, at 15 dpi, *MgumB* cankers on RNAi*CaIS1* leaves were noticeably different from wild-type *Xcc* cankers. *MgumB* cankers displayed isolated microcolonies of bacteria dispersed within the cankers, suggesting an interruption or nonprogression of canker development (Figure 4e). In comparison, wild-type *Xcc* cankers were fully developed (demonstrated visually by solid fluorescence), and slightly larger in size even compared to the cankers that formed on wild-type plants (Figure 4b, e). Wild-type and RNAi*CaIS1* plants inoculated with 10 mM $MgCl_2$ served as controls and showed no symptoms (data not shown).

To assess the bacterial growth kinetics in RNAi*CaIS1* plants and wild-type plants, leaves were inoculated with bacterial suspensions of the *Xcc* and *gumB* mutant as described previously. In wild-type plants, the population size of the *gumB* mutant was significantly lower than *Xcc*, as expected from previous work (Rigano *et al.*, 2007) (Figure 4c). Comparison

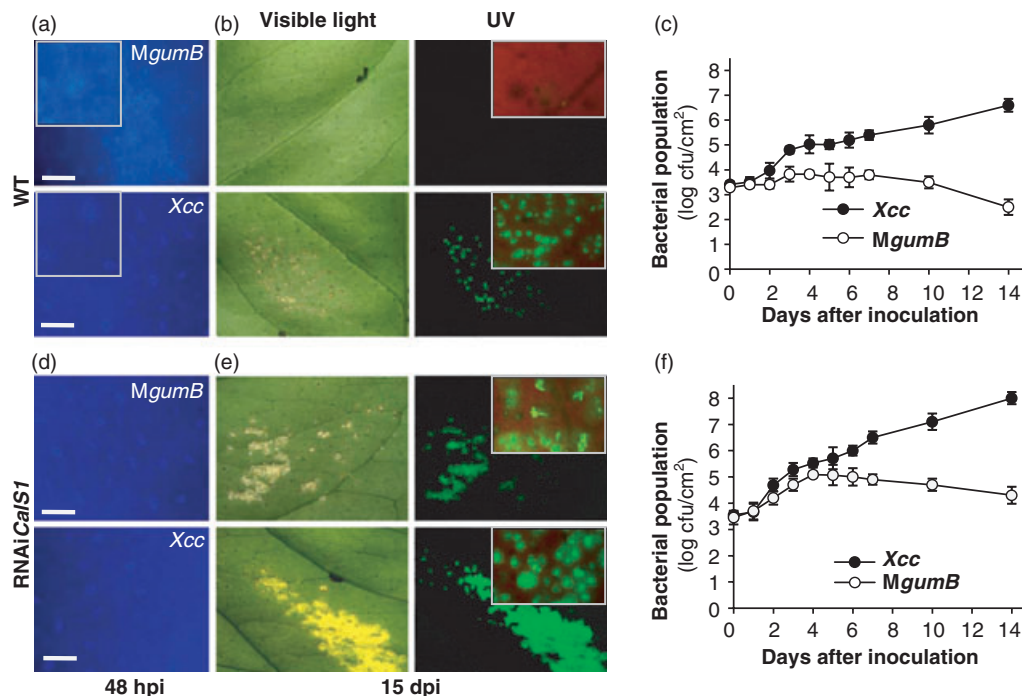


Figure 4 Silencing of *CaIS1* in *C. limon* increases susceptibility to *Xanthomonas*. (a, d) *MgumB* and *Xcc* strains were inoculated onto wild-type (WT) and RNAi*CaIS1* leaves and were stained with aniline blue at 48- h postinoculation (hpi) to detect callose deposition. Insets show amplification of the callose staining (bright-light blue dots). Scale bars 100 μ m. (b, e) Symptom development induced by wild-type strain of *Xcc*-GFP and *MgumB*-GFP strain on lower surfaces of wild-type (WT) and RNAi*CaIS1* lemon leaves 15 dpi. Leaves were photographed under white and UV light (520 nm), respectively. GFP-labelled bacteria within the canker pustule are shown enlarged in the top inset. (c, f) Growth *in vivo* of *Xcc* and *MgumB* strains on wild-type (WT) and RNAi*CaIS1* leaves, respectively. Values are expressed as means \pm standard deviation of three independent experiments.

of bacterial numbers in RNAi*CalS1* plants, however, revealed no significant differences between the growth of the *Xcc* and *gumB* mutant up to 4–6 dpi. After that time, the population of the *gumB* mutant began to decline and no mutant bacteria could be recovered after 4–5 weeks (data not shown). These results are consistent with the canker symptoms developed by *gumB* mutant on RNAi*CalS1* plants (Figure 4e). Furthermore, the population size of both strains was more than one order of magnitude greater in silenced plants compared to wild-type plants over the 14-day monitoring period (Figure 4f).

CalS1 activity in citrus is insufficient for defence against the xanthan-deficient *Xcc gumB* mutant

We have shown that xanthan produced by *Xcc* suppresses pathogen-associated molecular patterns (PAMPs)-induced signalling in wild-type *C. limon* leaves (Figure 4a, d). To gain better understanding of the defence responses that makes callose-deficient plants more susceptible to *Xcc* infection, we analysed other early host defence markers, including reactive oxygen species levels, measured as hydrogen peroxide. A high accumulation of H₂O₂ in wild-type lemon plants inoculated with the xanthan-deficient *gumB* mutant was observed at 15-h postinoculation, maintaining high levels until 5 dpi (Figure 5a). Interestingly, RNAi*CalS1* leaves inoculated with *MgumB* show a H₂O₂ pattern that is similar to the pattern observed in wild-type plants inoculated with this mutant (Figure 5a). At the beginning of *MgumB* infection, both plants showed higher H₂O₂ accumulation within the guard cells of the stomata, which represent an important entry route for *Xcc*. At 5 dpi with *MgumB*, H₂O₂ production was also observed in the apoplast, which is where *Xcc* wild-type multiplies. The number and intensity of the green fluorescent spots induced by *MgumB* visualized with the H₂O₂-sensitive dye DCFH-2DA was greatly increased both in control wild-type ($48.3 \pm 6.4\%$) and RNAi*CalS1* ($52.1 \pm 5.8\%$) plants. No H₂O₂ accumulation was observed in wild-type ($0.076 \pm 0.018\%$) and RNAi*CalS1* ($0.081 \pm 0.015\%$) leaves inoculated with *Xcc* (Figure 5a). This result confirms that bacterial xanthan production suppresses *Xcc* elicitor-triggered immunity in citrus plants.

To clarify the relationship between accumulation of H₂O₂ and bacterial epiphytic fitness, we analysed the population size of *Xcc* and *MgumB* on the surface of wild-type and RNAi*CalS1* lemon leaves at 5 days postinoculation. As shown in Figure 5b, the population size of *gumB* mutant was much smaller compared to the *Xcc* population

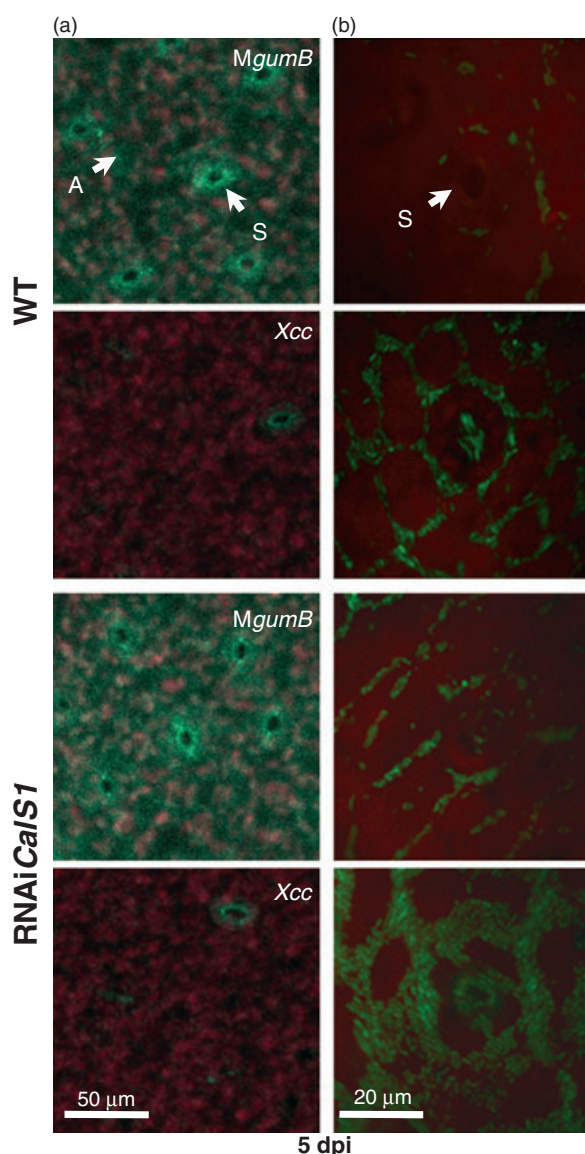


Figure 5 The accumulation of H₂O₂ triggered by the xanthan-deficient mutant (*MgumB*) does not require *CalS1* expression. (a) *MgumB* and *Xcc* strains were inoculated onto wild-type (WT) and RNAi*CalS1* leaves and stained with 2',7'-dichlorofluorescein diacetate to detect H₂O₂ accumulation at 5 days postinoculation (dpi). Leaves were photographed using confocal laser scanning microscopy. Red indicates chlorophyll autofluorescence. Magnification 50×; Scale bars, 50 μm. (b) Epiphytic population of *Xcc* and the *MgumB* mutant on superficial lemon leaf at 5 dpi. GFP-labelled bacteria were detected by fluorescence microscopy. Magnification 100×; Scale bars, 20 μm. Four independent biological assays were carried out for each strain using five wild-type and five RNAi*CalS1* plants (three leaves per plant) with essentially the same outcome. Stomata (S) and apoplast (A) are indicated by arrows.

size across both wild-type and RNAi*CalS1* leaves, and both leaf types displayed higher H₂O₂ levels following inoculation with the *MgumB* mutant compared to inoculation

with *Xcc*. Irrespective of bacterial strain, more aggregates were seen on RNAiCa/S1 leaves than on wild-type leaves at early stages postinfection. These results are consistent with the results shown in Figure 4 and suggest that callose deposition is a rapid and specific cell wall response during *Xcc* infection.

Taken together, these findings indicate a greater susceptibility of RNAiCa/S1 plants compared with wild-type plants to *Xcc*, confirming a role for CalS1 in callose synthesis during citrus defence against this pathogen. However, these findings also suggest that without bacterial xanthan production, inhibition of callose deposition is not enough to allow bacterial growth, as evidenced by the limited growth of the *MgumB* mutant on RNAiCa/S1 leaves. A likely explanation is that in the absence of callose deposition, other defence signalling molecules or signalling triggered by H₂O₂ itself are eventually able to contain the pathogen (Quan *et al.*, 2008). This does not occur with the wild-type *Xcc* strain because xanthan successfully suppresses the defence response.

Discussion

An optimized method for RNAi induction in citrus via hpRNA expression

Gene silencing by transient expression of RNAi-inducing hairpin RNA does not require stable genetic transformation and is consequently a very promising technique for functional genomic analysis in citrus. In this work, we optimized the hpRNA silencing system (Wesley *et al.*, 2001; Helliwell and Waterhouse, 2003) in *C. limon* and other members of the *Rutaceae* family to allow for functional analysis of candidate genes. We first evaluated the silencing system using lemon endogenous *PDS*, a gene that has been used for this purpose in many plant species (Kumagai *et al.*, 1995; Ruiz *et al.*, 1998; Liu *et al.*, 2002; Brigneti *et al.*, 2004). Upon induction of *PDS* silencing with these constructs, we observed different grades of photobleaching. Plants most severely afflicted died following complete photobleaching. In milder cases, silencing in the upper leaves did not persist and only leaves from one new lateral branch displayed photobleaching after pruning (Figure 1). Approximately 80% of silenced plants showed a strong photobleaching phenotype in systemic leaves that persisted for at least a year postinoculation (Figure 1). The demonstrated success of *PDS* systemic silencing in citrus provides a basis for analysis of citrus gene function, metabolic routes and signalling pathways using RNAi.

Role of callose in citrus development

We exploited the high-throughput capability of the hairpin RNA vector and the availability of partial *C. reschii* CalS cDNA library to test possible roles for this gene in cell wall development and defence responses to *Xcc* in lemon plants.

RNAiCa/S1 *C. limon* plants were generated by transient expression of hpRNA from the pHG12 *CI-CalS1* vector, which contains the endogenous *C. limon* CalS1 target gene sequence (Figure 2). In these systemic silencing leaves, expression of the construct reduced CalS1 mRNA levels to 20% tested by qRT-PCR. This can be explained by the accumulation of CalS1 21 nt siRNAs (Figure 3) (Hamilton and Baulcombe, 1999; Hamilton *et al.*, 2002). As shown in Figures 2 and 3, RNAiCa/S silencing citrus plants led to alterations at both gross phenotypical and histological levels. Silenced plants were shorter than control plants and their leaves were wrinkled and smaller. A similar phenotype was reported in cellulose synthase-silenced *N. benthamiana* (Burton *et al.*, 2000). Recently, it was reported that CalS1 gene expression is regulated in a tissue-specific manner in both the leaves and root hairs of *Arabidopsis* (Dong *et al.*, 2008). Histological analysis of RNAiCa/S1 *C. limon* leaves showed morphological alterations both in shape and organization of cells. It was suggested that the formation of a functional CalS1 complex is vital to building a cell plate, which must be completed in a short time, and that imbalanced synthesis of callose may alter the composition of the cell plate producing daughter cells with altered cell walls (Verma and Hong, 2001). We hypothesize that these alterations are caused by a temporary loss of cell wall strength or rigidity enabling abnormal cell expansion in lemon leaves.

CalS1 is required to defend against *Xcc* infection in citrus plants

The greater susceptibility of RNAiCa/S1 plants to *Xcc* compared to wild-type plants suggests that CalS1 plays a role in citrus defence against this pathogen (Figure 4). Recently, Lee *et al.* (2009) studied the ultrastructural aspects of citrus canker development in unwounded leaves of citrus species. They showed that in leaves from the susceptible species of Mexican lime, *Xcc* invasion and extracellular multiplication were usually accompanied by host cell wall dissolution and a disruption of the host cell. Local accumulation of papillae-like materials within the host cells and in close proximity to bacteria was observed in the

mesophyll tissues of more resistant species, such as Yuzu (*C. ichangensis* X *C. reticulata* var. *austere*). Based on our findings and the results obtained by Lee *et al.* (2009), we propose that callose contributes to penetration resistance against invading bacterial mesophyll pathogens by providing a physical barrier. In callose-silenced citrus plants, the consequent reduction in callose levels may weaken this barrier leading to enhanced Xcc susceptibility compared to wild-type plants.

Recently, Dong *et al.* (2008) reported a significant induction of *CalS1* and *CalS12* genes in *Arabidopsis* by salicylic acid treatment and upon *Hyaloperonospora arabidopsis* infection. Interestingly, the *cals12* *Arabidopsis* mutant not only failed to synthesize callose at papillae but was also more resistant to the fungus compared to the *cals1* *Arabidopsis* mutant and wild-type plants (Dong *et al.*, 2008). These surprising results are consistent with the two other recent reports on *Arabidopsis pmr4/gsl5* (*cals12*) mutants (Jacobs *et al.*, 2003; Nishimura *et al.*, 2003), in which these plants were found to be more resistant to fungi powdery mildew and downy mildew. In contrast, Vogel and Somerville (2000) observed greater susceptibility in *Arabidopsis* using the fungus *Erysiphe cichoracearum*. To explain these seemingly contradictory findings, it has been proposed that pathogen-induced callose may negatively regulate the salicylic acid signalling pathway of the plant and that the lack of callose in these mutants may therefore suppress pathogen infection (Nishimura *et al.*, 2003; Dong *et al.*, 2008).

Taken together, these results suggest that different CalS isoforms may be required for callose production in specific tissues and that callose may play multiple roles depending on the pathogen and host.

Death of *MgumB* mutant is because of oxidative burst rather than callose deposition

Xanthan plays an important role in biofilm formation and canker development on lemon leaves (Rigano *et al.*, 2007). Here, we have shown that the reduced virulence of *MgumB*, associated with the lack of xanthan, correlates not only with callose deposition but also with high generation of H₂O₂ in wild-type plants (Figures 4 and 5). These results suggest that another role of xanthan in bacterial canker disease is to suppress defence induction in citrus, which supports earlier findings on the role of callose in plant defence to bacterial pathogens (Yun *et al.*, 2006; Aslam *et al.*, 2008).

Surprisingly, the canker symptoms induced by the *gumB* mutant on RNAi*CalS1* lemon leaves at 15 dpi were not fully developed (Figure 4). This correlates with the low cell number observed on the leaf surface of these plants at an earlier time postinfection (Figure 5b). Moreover, plants inoculated with the xanthan-deficient mutant failed to induce callose deposition, but showed no alteration in H₂O₂ production (Figures 4 and 5).

Together, these results indicate that *MgumB* can colonize RNAi*CalS1* tissue, but that without xanthan the bacteria are unable to survive for a long period (e.g. beyond 30–35 days) and that defence triggering induced by PAMPs kills the bacteria. The different outcome of the *MgumB* mutant compared to wild-type Xcc may reflect the multiple roles of xanthan in plant disease. Possible roles may include contribution to bacterial survival within leaves, for example through biofilm formation, the ability to retain water and resistance to abiotic stress (Rigano *et al.*, 2007), as well as suppression of additional plant defence responses, such as callose deposition and H₂O₂ accumulation.

In conclusion, we have developed an efficient method to study gene function in *C. limon* using agroinfiltration to transiently silence endogenous genes. The silencing approach should allow further study of the function of genes in citrus beyond the *CalS* gene family. Currently, an abundance of citrus ESTs are available in a public database, covering an array of citrus varieties and responses to abiotic and biotic stresses (International Citrus Genome/Genomics Consortium, <http://www.citrusgenome.ucr.edu/>). This sequence availability, combined with the successful hpRNA vector in *C. limon* demonstrated here, should facilitate the study of gene function in citrus interactions not only with Xcc but also with a range of other pathogens. Moreover, knocking out the expression of host genes with a role in canker disease will likely be an important tool in development of new and sustainable strategies to manage the disease.

Experimental procedures

Plant material, pathogens and pathogenicity assays

Plantlets from seed germination of *Citrus lemon* (L.) Burm f. (cv. Eureka Frost and cv. Lisboa Frost) and Troyer citrange (*Poncirus trifoliata* (L.) Raf. x *Citrus sinensis* (L.) Osb.) were used for silencing assays. Seeds were collected in Tucumán and provided by the Estación Experimental Agroindustrial Obispo Colombres, Tucumán, Argentina. After disinfection with 0.5% v/v of sodium hypochlorite for 15 min, seeds were germinated in a 1 : 1 mixture

of compost and peat. The plantlets were grown as previously reported (Siciliano *et al.*, 2006). Propagation of silencing was evaluated by grafting buds of silenced lemon plantlets onto non-silenced Troyer citrange rootstocks using the grafting standard procedure. Average grafting success was 30–50% from 30 grafts. Grafted plants were acclimatized in a greenhouse and were tested 3–6 months after the bud break for the silenced phenotype.

The GFP-labelled bacteria of *Xanthomonas citri* subsp. *citri* (Xcc) wild-type strain and the mutant strain defective in production of the extracellular polysaccharide xanthan, Xcc *gumB* (MgumB), were previously described (Rigano *et al.*, 2007). Bacterial suspensions of Xcc and *gumB* mutants (10^7 cfu/mL in 10 mM MgCl₂) were inoculated onto the surface of lemon leaves by cotton swab. Inoculated plants were maintained for 25–30 days in a growth cabinet, with temperatures ranging from 25 to 28 °C, high humidity, a photoperiod of 16-h light and a light intensity of 150–200 $\mu\text{E/s/m}^2$. Disease progression was monitored phenotypically in three separate biological assays and through analysis of bacterial growth curves (Rigano *et al.*, 2007).

Construction of hairpin RNA expression vectors

The pHELLSGATE12 vector (CSIRO Plant Industry, Camberra, Australia) (Helliwell and Waterhouse, 2003) and the Gateway recombination system from Invitrogen (<http://www.invitrogen.com/gateway>) were used to generate the RNAi constructs, whereby a PCR product amplified from the target gene is first inserted into the donor pENTR3C vector (Invitrogen, Carlsbad, CA, USA) between *attL1/attL2* sites. The gene fragment from the intermediate clone is then inserted into the pHELLSGATE12 vector by recombination between *attL1/attL2* and *attR1/attR2*, mediated by LR Clonase (Invitrogen). When the construct is expressed in plants, a hairpin RNA (hpRNA) with the intron spliced out is produced.

Fragments of 386 bp from the *Citrus limon* phytoene desaturase (*CI-PDS*) coding region were PCR amplified using the primer pairs, 5'-GCCATGTCAAAGGCACTAAA-3' (PDS-R) and 5'-ATGACTGGAAGTCCCACCAA-3' (PDS-F), designed from *PDS* ESTs sequences of *C. sinensis* (DQ235261). The fragments of 398 bp from the *C. limon* callose synthase (*CI-CalS*) coding region were PCR amplified using the primer pairs, 5'-CCGCCATAAAGAAACACAT-3' (CalS-R) and 5'-CCGCCATAAAGAAACACAT-3' (CalS-F), designed from *CalS* ESTs sequences of *C. reshni* (CX305437). The *CI-PDS* and *CI-CalS* PCR products were purified and cloned into the pGEM-T Easy vector (Promega, Mannheim, Germany) to produce pGEM *CI-PDS* and pGEM *CI-CalS*, respectively. These constructs were then sequenced, digested with *EcoRI* and sub-cloned into the cleavage site, *EcoRI*, of the pENTR3C vector (Invitrogen). Recombination reactions from pENTR *CI-PDS* and pENTR *CI-CalS* clones with pHELLSGATE12 vector were carried out according to Helliwell and Waterhouse (2003). Transformed *Escherichia coli* DH5 α cells were selected on LB media (Sambrook *et al.*, 1989) supplemented with 100 $\mu\text{g/mL}$ spectinomycin. The presence and orientation of the insert was confirmed by restriction digest with *XhoI* and *XbaI* of the plasmid DNA (Helliwell and Waterhouse, 2003). Between 70% and 80% of the clones obtained contained the pyruvate dehydrogenase kinase (PDK) intron in reverse orientation (pHG12 *CI-TARGET GENE-R*) with respect to the promoter. The remaining 20% contained the intron in forward orientation (pHG12 *CI-TARGET GENE-F*).

Agroinfiltration-mediated delivery of dsRNAs

Agrobacterium tumefaciens EHA105 cells (Hood *et al.*, 1993) transformed by electroporation (Dower *et al.*, 1988) with either the pHG12 *CI-PDS* construct or the pHG12 *CI-CalS1* construct were inoculated into 10 mL of LB medium (Sambrook *et al.*, 1989) supplemented with 25 $\mu\text{g/mL}$ nalidixic acid and 100 $\mu\text{g/mL}$ spectinomycin and grown at 28 °C to saturation. Cells were precipitated and resuspended to a final concentration of 0.8 OD₆₀₀ in a solution containing 10 mM MgCl₂ and 150 μM acetosyringone (Sigma-Aldrich, St Louis, MO). The cultures were incubated at room temperature for 6 h before agroinfiltration. The agroinfiltration into *C. limon* plants at the four- to six-leaf stage was performed as described previously (Siciliano *et al.*, 2006). Each construct was infiltrated into five plants grown from seeds.

Real-time quantitative reverse transcription-PCR

Total RNA from control and silenced lemon leaves was isolated according to the manufacturer's instructions (RNeasy Plant Mini Kit; Qiagen, Valencia, CA), following treatment with RNase-free DNase (Promega, Mannheim, Germany). Reverse transcription was performed by M-MLV reverse transcriptase (Invitrogen) with 1 μg DNase-treated total RNA and oligo-dT12-18 as primers. Synthesized cDNA was used for quantitative reverse transcription-polymerase chain reaction (qRT-PCR). The reactions were carried out in the presence of the double-stranded DNA-specific dye SYBR green (Invitrogen) and monitored in real time with the Mastercycler ep *realplex* real-time PCR system (Eppendorf, Hamburg, Germany). The following oligonucleotides were used in this study: *PDS*: PDS-F and PDS-R; *CalS*: CalS-F and CalS-R. A lemon actin amplicon used as internal standard for quantifications was amplified using 5'-TTTACCACCACAGCCGAACG-3' (ACT-R) and 5'-TGGAGCCACGACCTTGAT-3' (ACT-F). All of these amplicons have a product size approximately of 400 bp. PCRs were performed for 40 cycles according to the following conditions: denaturation at 95 °C for 15 s, annealing at 55 °C for 30 s and extension at 72 °C for 40 s. After amplification, melting-curve analyses were performed to exclude artefactual amplifications. The relative expression of transcripts RNA was calculated using the threshold cycle values (Ct) obtained from each sample as follows: relative expression = $2^{-\Delta\Delta\text{Ct}}$, being $\Delta\text{Ct} = \text{Ct}_{\text{sample}} - \text{Ct}_{\text{actin}}$ and $\Delta\Delta\text{Ct} = \Delta\text{Ct}_{\text{sample}} - \Delta\text{Ct}_{\text{ref sample}}$. Nonsilenced lemon leaves served as the reference sample, and the results were normalized against actin. The average values were calculated from triplicate samples.

Small RNA Northern blot

Total RNA from *Citrus limon* leaves was isolated using TRIzol reagent (Invitrogen) followed by separation on 17.5% denaturing polyacrylamide gels. RNAs were transferred to Hybond N+ membrane (Amersham Pharmacia Biotech, Bucks, UK) in TBE 0.5 \times for 1 h using the Bio-Rad semi-dry transfer unit at 300 mA at 25 °C. Membranes were fixed by UV cross-linking at 1200 $\mu\text{Joules} \times 100$ (UVP UV Crosslinker, UK). The blots were hybridized with [α -³²P] ATP-labelled DNA probes of *CI-CalS* generated by random priming

from the respective cDNA clones. Both prehybridization and hybridization reactions were performed as described in Hamilton and Baulcombe (1999) at 40 °C. Radioactivity in bands was detected using a phosphorimager Storm 840 (Amersham Pharmacia Biotech, Bucks, UK).

Histological and anatomical assays

Citrus limon plants agro-infiltrated with either pHG12 *CI-CalS1* or *Agrobacterium* EHA105 alone were photographed at 50 days post-inoculation. The internode length was measured with the ImageJ software v1.41 (National Institutes of Health, Bethesda, MD, USA). Data were analysed with analysis of variance (one-way ANOVA). This analysis was carried out with five RNAiCalS1 plants and five control wild-type plants in three replicate experiments.

Histological staining employed young leaves (50%–80% expansion) that were cut from 60-day-old *CalS1*-silenced and wild-type plants. All materials were immediately immersed in a fixative containing 10% formaldehyde, 5% acetic acid and 50% ethanol. After the material was dehydrated through a graded ethanol series, the leaves were passed through graded solutions of xylene in absolute ethanol and immersed in several changes of melted paraffin in xylene (65 °C) (Berlyn and Miksche, 1976). The paraffin-embedded samples were traced on 10- µm-thick paraffin sections, using a Minot 1212 microtome (Leitz, Wetzlar, Germany). The tissues were stained with safranin and fast-green and mounted in Canada balsam (Strittmatter, 1979).

H₂O₂ and callose detection

Histochemical detection of H₂O₂ was carried out as described by Sanchez *et al.* (2010) after staining with fluorescence marker 2',7'-dichlorofluorescein diacetate (DCFH-DA; Sigma-Aldrich) (Ezaki *et al.*, 2000). H₂O₂ accumulation was quantified by comparing the number of green fluorescent pixels following *MgumB* inoculation to the number of green fluorescent pixels following *Xcc* inoculation relative to the total pixel count on digital photographs of treated leaf areas using the program ImageJ software v1.41 (National Institute of Health). The experiment was repeated on at least five different plants, and three leaves per plant were examined and photographed under UV light with an inverted confocal microscope (Nikon C1, Japan). The images were generated by using Nikon EZ-C1 Version 3.90. Aniline blue staining for the presence of callose deposition in *C. limon* leaves was performed as described previously (Yun *et al.*, 2006). Leaves were examined and photographed under UV light with an epifluorescence microscope (BH2; Olympus Optical Ltd. Company, Tokyo, Japan).

Acknowledgements

This work was supported by the Agencia de Promoción Científica y Tecnológica (PAV-137; PICT-2007-00469) and Consejo Nacional de Investigaciones Científicas y Técnicas (CONICET, PIP6441) to M. R. Marano. We express our sincere thanks to P. Waterhouse of CSIRO, Australia for

distributing pHELLSGATE12 vector, Adriana Cortadi, Alejandra Ines Martinez and Abelardo Vegetti for the generous help in the preparation and analysis of the histological leaf tissues and Sonia Scarpeci for her technical assistance with the confocal microscope. We also thank J. Maxwell Dow and Maureen Richey for critically reading the manuscript. M.R.M, A.A.V and A.P.C are Career Investigators of the CONICET.

References

- Aslam, S.N., Newman, M.A., Erbs, G., Morrissey, K.L., Chinchilla, D., Boller, T., Jensen, T.T., De Castro, C., Ierano, T., Molinaro, A., Jackson, R.W., Knight, M.R. and Cooper, R.M. (2008) Bacterial polysaccharides suppress induced innate immunity by calcium chelation. *Curr. Biol.*, **18**, 1078–1083.
- Berlyn, G.P. and Miksche, J.B. (1976) *Botanical microtechnique and citochemistry*. 2nd edn, Ames, IA: Iowa State University Press, 326.
- Brigneti, G., Martin-Hernandez, A.M., Jin, H., Chen, J., Baulcombe, D.C., Baker, B. and Jones, J.D. (2004) Virus-induced gene silencing in *Solanum* species. *Plant J.*, **39**, 264–272.
- Burton, R.A., Gibeaut, D.M., Bacic, A., Findlay, K., Roberts, K., Hamilton, A., Baulcombe, D.C. and Fincher, G.B. (2000) Virus-induced silencing of a plant cellulose synthase gene. *Plant Cell*, **12**, 691–706.
- Campos, M.A., Rosa, D.D., Teixeira, J.E.C., Targon, M.L.P.N., Souza, A.A., Paiva, L.V., Stach-Machado, D.R. and Machado, M.A. (2007) *PR* gene family of citrus: their organ specific-biotic and abiotic inducible expression based on ESTs approach. *Genet. Mol. Biol.*, **30**, 917–930.
- Cernadas, R.A., Camillo, L.R. and Benedetti, C.E. (2008) Transcriptional analysis of the sweet orange interaction with the citrus canker pathogens *Xanthomonas axonopodis* pv. *citri* and *Xanthomonas axonopodis* pv. *aurantifolii*. *Mol. Plant Pathol.*, **9**, 609–631.
- Chen, X.Y. and Kim, J.Y. (2009) Callose synthesis in higher plants. *Plant Signal Behav.*, **4**, 489–492.
- Cristofani-Yaly, M., Berger, I.J., Targon, M.L.P.N., Takita, M.A., Dorta, S.O., Freitas-Astua, J., Souza, A.A., Boscariol-Camargo, R.L., Reis, M.S. and Machado, M.A. (2007) Differential expression of genes identified from *Poncirus trifoliata* tissue inoculated with CTV through EST analysis and *in silico* hybridization. *Genet. Mol. Biol.*, **30**, 972–979.
- Dong, X., Hong, Z., Chatterjee, J., Kim, S. and Verma, D.P. (2008) Expression of callose synthase genes and its connection with Npr1 signaling pathway during pathogen infection. *Planta*, **229**, 87–98.
- Dower, W.J., Miller, J.F. and Ragsdale, C.W. (1988) High efficiency transformation of *E. coli* by high voltage electroporation. *Nucleic Acids Res.*, **16**, 6127–6145.
- Enns, L.C., Kanaoka, M.M., Torii, K.U., Comai, L., Okada, K. and Cleland, R.E. (2005) Two callose synthases, GSL1 and GSL5, play an essential and redundant role in plant and pollen development and in fertility. *Plant Mol. Biol.*, **58**, 333–349.

- Ezaki, B., Gardner, R.C., Ezaki, Y. and Matsumoto, H. (2000) Expression of aluminum induced genes in transgenic *Arabidopsis* plants can ameliorate aluminum stress and/or oxidative stress. *Plant Physiol.*, **122**, 657–666.
- Forment, J., Gadea, J., Huerta, L., Abizanda, L., Agusti, J., Alamar, S., Alos, E., Andres, F., Arribas, R., Beltran, J.P., Berbel, A., Blazquez, M.A., Brumos, J., Canas, L.A., Cercos, M., Colmenero-Flores, J.M., Conesa, A., Estables, B., Gandia, M., Garcia-Martinez, J.L., Gimeno, J., Gisbert, A., Gomez, G., Gonzalez-Candelas, L., Granell, A., Guerri, J., Lafuente, M.T., Madueno, F., Marcos, J.F., Marques, M.C., Martinez, F., Martinez-Godoy, M.A., Miralles, S., Moreno, P., Navarro, L., Pallas, V., Perez-Amador, M.A., Perez-Valle, J., Pons, C., Rodrigo, I., Rodriguez, P.L., Royo, C., Serrano, R., Soler, G., Tadeo, F., Talon, M., Terol, J., Trenor, M., Vaello, L., Vicente, O., Vidal, Ch., Zacarias, L. and Conejero, V. (2005) Development of a citrus genome-wide EST collection and cDNA microarray as resources for genomic studies. *Plant Mol. Biol.*, **57**, 375–391.
- Freitas-Astua, J., Bastianel, M., Locali-Fabris, E.C., Novelli, V.M., Silva-Pinhati, A.C., Basilio-Palmieri, A.C., Targón, M.L.P.N. and Machado, M.A. (2007) Differentially expressed stress-related genes in the compatible citrus-Citrus leprosis virus interaction. *Genet. Mol. Biol.*, **30**, 980–990.
- Gandia, M., Conesa, A., Ancillo, G., Gadea, J., Forment, J., Pallas, V., Flores, R., Duran-Vila, N., Moreno, P. and Guerri, J. (2007) Transcriptional response of *Citrus aurantifolia* to infection by *Citrus tristeza virus*. *Virology*, **367**, 298–306.
- Gmitter Jr, F.G. (1995) Origin, evolution and breeding of the grapefruit. In *Plant Breeding Reviews*, (Janick, J. ed.), vol. 13, pp. 345–363, New York, USA: John Wiley & Sons.
- Graham, J.H., Gottwald, T.R., Cubero, J. and Achor, D.S. (2004) *Xanthomonas axonopodis* pv. *citri*: factors affecting successful eradication of citrus canker. *Mol. Plant Pathol.*, **1**, 1–15.
- Hamilton, A.J. and Baulcombe, D.C. (1999) A species of small antisense RNA in posttranscriptional gene silencing in plants. *Science*, **286**, 950–952.
- Hamilton, A., Voinnet, O., Chappell, L. and Baulcombe, D. (2002) Two classes of short interfering RNA in RNA silencing. *EMBO J.*, **21**, 4671–4679.
- Helliwell, C. and Waterhouse, P. (2003) Constructs and methods for high-throughput gene silencing in plants. *Methods*, **30**, 289–295.
- Hong, Z., Delauney, A.J. and Verma, D.P. (2001) A cell plate-specific callose synthase and its interaction with phragmoplastin. *Plant Cell*, **13**, 755–768.
- Hood, E.E., Gelvin, S.B., Melchers, L.S. and Hoekema, A. (1993) New *Agrobacterium* helper plasmids for gene transfer to plants. *Transgenic Res.*, **2**, 208–218.
- Jacobs, A.K., Lipka, V., Burton, R.A., Panstruga, R., Strizhov, N., Schulze-Lefert, P. and Fincher, G.B. (2003) An *Arabidopsis* callose synthase, GSL5, is required for wound and papillary callose formation. *Plant Cell*, **15**, 2503–2513.
- Khalaf, A., Moore, G.A., Jones, J.B. and Gmitter Jr F.G. (2007) New insights into the resistance of Nagami kumquat to canker disease. *Physiol. Mol. Plant Pathol.*, **71**, 240–250.
- Kumagai, M.H., Donson, J., della-Cioppa, G., Harvey, D., Hanley, K. and Grill, L.K. (1995) Cytoplasmic inhibition of carotenoid biosynthesis with virus-derived RNA. *Proc. Natl. Acad. Sci. USA*, **92**, 1679–1683.
- Lahey, K.A., Yuan, R., Burns, J.K., Ueng, P.P., Timmer, L.W. and Kuang-Ren, C. (2004) Induction of phytohormones and differential gene expression in citrus flowers infected by the fungus *Colletotrichum acutatum*. *Mol. Plant Microbe Interact.*, **17**, 1394–1401.
- Lee, I.J., Kim, K.W., Hyun, J.W., Lee, Y.H. and Park, E.W. (2009) Comparative ultrastructure of nonwounded Mexican lime and Yuzu leaves infected with the citrus canker bacterium *Xanthomonas citri* pv. *citri*. *Microsc. Res. Tech.*, **72**, 507–516.
- Liu, Y., Schiff, M. and Dinesh-Kumar, S.P. (2002) Virus-induced gene silencing in tomato. *Plant J.*, **31**, 777–786.
- Marcos, J.F., Gonzalez-Candelas, L. and Zacarias, L. (2005) Involvement of ethylene biosynthesis and perception in the susceptibility of citrus fruits to *Penicillium digitatum* infection and the accumulation of defence-related mRNAs. *J. Exp. Bot.*, **56**, 2183–2193.
- Marques, M.C., Alonso-Cantabrana, H., Forment, J., Arribas, R., Alamar, S., Conejero, V. and Perez-Amador, M.A. (2009) A new set of ESTs and cDNA clones from full-length and normalized libraries for gene discovery and functional characterization in citrus. *BMC Genomics*, **10**, 428.
- Martinez-Godoy, M.A., Mauri, N., Juarez, J., Marques, M.C., Santiago, J., Forment, J. and Gaeda, J. (2008) A genome-wide 20 K citrus microarray for gene expression analysis. *BMC Genomics*, **9**, 318.
- Nishimura, M.T., Stein, M., Hou, B.H., Vogel, J.P., Edwards, H. and Somerville, S.C. (2003) Loss of a callose synthase results in salicylic acid-dependent disease resistance. *Science*, **301**, 969–972.
- Quan, L.J., Zhang, B., Shi, W.W. and Li, H.Y. (2008) Hydrogen peroxide in plants: a versatile molecule of the reactive oxygen species network. *J. Integr. Plant Biol.*, **50**, 2–18.
- Richmond, T.A. and Somerville, C.R. (2000) The cellulose synthase superfamily. *Plant Physiol.*, **124**, 495–498.
- Rigano, L.A., Siciliano, F., Enrique, R., Sendin, L., Filippone, P., Torres, P.S., Questa, J., Dow, J.M., Castagnaro, A.P., Vojnov, A.A. and Marano, M.R. (2007) Biofilm formation, epiphytic fitness, and canker development in *Xanthomonas axonopodis* pv. *citri*. *Mol. Plant Microbe Interact.*, **20**, 1222–1230.
- Ruiz, M.T., Voinnet, O. and Baulcombe, D.C. (1998) Initiation and maintenance of virus-induced gene silencing. *Plant Cell*, **10**, 937–946.
- Sambrook, J., Fritsch, E.F. and Maniatis, T. (1989) *Molecular Cloning: A Laboratory Manual*, 2nd edn, New York, USA: Cold Spring Harbor: Cold Spring Harbor Laboratory Press.
- Samuels, A.L., Giddings, T.H. Jr and Staehelin, L.A. (1995) Cytokinesis in tobacco BY-2 and root tip cells: a new model of cell plate formation in higher plants. *J. Cell Biol.*, **130**, 1345–1357.
- Sanchez, G., Gerhardt, N., Siciliano, F., Vojnov, A., Malcuit, I. and Marano, M.R. (2010) Salicylic acid is involved in the Nb-mediated defense responses to potato virus X in *Solanum tuberosum*. *Mol. Plant Microbe Interact.*, **23**, 394–405.
- Schaad, N.W., Postnikova, E., Lacy, G., Sechler, A., Agarkova, I., Stromberg, P.E., Stromberg, V.K. and Vidaver, A.K. (2006) Emended classification of xanthomonad pathogens on citrus.

- Syst. Appl. Microbiol.* **2**, 690–695. doi: 10.1016/j.syapm.2006.08.001.
- Schubert, T.S., Rizvi, S.A., Sun, X.A., Gottwald, T.R., Graham, J.H. and Dixon, W.N. (2001) Meeting the challenge of eradicating citrus canker in Florida-again. *Plant Dis.*, **85**, 340–356.
- Shiotani, H., Uematsu, H., Tsukamoto, T., Shimizu, Y., Ueda, K., Mizuno, A. and Sato, S. (2009) Survival and dispersal of *Xanthomonas axonopodis* pv. *citri* from infected Satsuma mandarin fruit. *Crop Prot.*, **28**, 19–23.
- Siciliano, F., Torres, P., Sendin, L., Bermejo, C., Filippone, P., Vellice, G., Ramallo, J., Castagnaro, A.P., Vojnov, A. and Marano, M.R. (2006) Analysis of the molecular basis of *Xanthomonas axonopodis* pv. *citri* pathogenesis in *Citrus limon*. *Electron. J. Biotechnol.*, **9**, 199–204.
- Souza, A., Takita, M., Coletta-Filho, H., Targon, M., Carlos, E., Locali-Fabris, E., Amaral, A.M., Freitas-Astúa, J., Silva-Pinhati, A.C.O., Boscariol-Camargo, R.L., Berger, I.J., Rodrigues, C.M., Reis, M.S. and Machado, M.A. (2007a) Analysis of expressed sequence tags from *Citrus sinensis* L. Osbeck infected with *Xylella fastidiosa*. *Genet. Mol. Biol.*, **30**, 957–964.
- Souza, A.A., Takita, M.A., Coletta-Filho, H.D., Campos, M.A., Teixeira, J.E.C., Targon, M.L.P.N., Carlos, E.F., Ravasi, J.F., Fischer, C.N. and Machado, M.A. (2007b) Comparative analysis of differentially expressed sequence tags of sweet orange and mandarin infected with *Xylella fastidiosa*. *Genet. Mol. Biol.*, **30**, 965–971.
- Strittmatter, C. (1979) Modificación de una técnica de coloración safranina-fast green. *Bol. Soc. Argent. Bot.*, **18**, 121–122.
- Tanaka, T. (1969) Misunderstanding with regards to *Citrus* classification and nomenclature. *Bull. Univ. Osaka Pref. Ser. B.*, **21**, 139–145.
- Targon, M.L.P.N., Takita, M.A., Amaral, A.M., Souza, A.A., Locali-Fabris, E.C., Dorta, S.O., Borges, K.M., Souza, J.M., Rodrigues, C.M., Luchetta, A.R., Freitas-Astua, J. and Machado, M.A. (2007) CitEST libraries. *Genet. Mol. Biol.*, **30**, 1019–1023.
- Terol, J., Conesa, A., Colmenero, J.M., Cercos, M., Tadeo, F., Agusti, J., Alos, E., Andres, F., Soler, G., Brumos, J., Iglesias, D.J., Gotz, S., Legaz, F., Argout, X., Courtois, B., Ollitrault, P., Dossat, C., Wincker, P., Morillon, R. and Talon, M. (2007) Analysis of 13000 unique citrus clusters associated with fruit quality, production and salinity tolerance. *BMC Genomics*, **8**, 31.
- Thiele, K., Wanner, G., Kindzierski, V., Jurgens, G., Mayer, U., Pachel, F. and Assaad, F.F. (2009) The timely deposition of callose is essential for cytokinesis in Arabidopsis. *Plant J.*, **58**, 13–26.
- Verma, D.P. and Hong, Z. (2001) Plant callose synthase complexes. *Plant Mol. Biol.*, **47**, 693–701.
- Vogel, J. and Somerville, S. (2000) Isolation and characterization of powdery mildew-resistant Arabidopsis mutants. *Proc. Natl. Acad. Sci. U S A*, **97**, 1897–1902.
- Wesley, S.V., Helliwell, C.A., Smith, N.A., Wang, M.B., Rouse, D.T., Liu, Q., Gooding, P.S., Singh, S.P., Abbott, D., Stoutjesdijk, P.A., Robinson, S.P., Gleave, A.P., Green, A.G. and Waterhouse, P.M. (2001) Construct design for efficient, effective and high-throughput gene silencing in plants. *Plant J.*, **27**, 581–590.
- Yun, M.H., Torres, P.S., El Oirdi, M., Rigano, L.A., Gonzalez-Lamothe, R., Marano, M.R., Castagnaro, A.P., Dankert, M.A., Bouarab, K. and Vojnov, A.A. (2006) Xanthan induces plant susceptibility by suppressing callose deposition. *Plant Physiol.*, **141**, 178–187.